Fault-Tolerant Control for Multi-Quadcopter with Suspended Payload under Wind Disturbance

Alif Al Farras
Department of Electrical Engineering
Institut Teknologi Sepuluh Nopember
Surabaya, Indonesia
alifalfarras@gmail.com

Ari Santoso
Department of Electrical Engineering
Institut Teknologi Sepuluh Nopember
Surabaya, Indonesia
santoso@ee.its.ac.id

Yurid Eka Nugraha
Department of Electrical Engineering
Institut Teknologi Sepuluh Nopember
Surabaya, Indonesia
yurid@its.ac.id

***Abstract*—Delivering payload with multiple quadcopters necessitates a reliable backup system. This research introduces a fault-tolerant design specifically for multi-drone payload transportation. The system employs formation control, ensuring the weight is evenly distributed among all functioning drones. This research tackles the challenge of reliable payload delivery with multi-drone systems. It proposes a new fault-tolerant control system specifically designed for this purpose. The system addresses a limitation in existing solutions by incorporating a simple PD controller alongside a fault-tolerant strategy. This approach allows the system to maintain operation even if a drone malfunctions. The paper further demonstrates the system's effectiveness through simulations. Results show the system's ability to maintain stability with minimal altitude loss (only 6.3cm) and rapid position reconfiguration (within 3.96 seconds) even under windy conditions. These findings highlight the potential of this fault-tolerant design to significantly improve multi-drone payload delivery, especially for missions requiring high levels of stability and redundancy.**

Keywords— fault-tolerant control, multi-UAVs, suspended payload, wind disturbances.

I. INTRODUCTION

In the latest technological era, the use of quadcopters is increasingly widespread and has become the focus of research in various fields. For example, a quadcopter is used to follow other objects [1], [2], [3], monitor an area [4],[5],[6], perform super fast maneuvers [7], [8],[9], form a circle formation on a target [10], track objects using multi-agents [11], [12], avoid obstacles [13], carry goods [14], fly in various conditions and terrain and so on. The main idea of this paper is to model a multi-quadcopter that transports loads simply but is also able to provide redundant features if one of the quadcopters does not work properly. This control system is crucial for enhancing the precision and accuracy of goods delivery, improving safety and security, meeting regulatory requirements, and expanding application opportunities. For example, consider a multi-quadcopter programmed to deliver emergency medicine to a remote area affected by a natural disaster. During the journey, one of the quadcopter's motors suddenly malfunctions. The fault-tolerant control system detects the failure and automatically adjusts the flight controls to compensate. The quadcopter continues to fly stably and delivers the medicine on time, saving many lives.

This paper utilizes a 6 DOF dynamic model of the quadcopter to design a PD controller for individual quadcopter movement control. Additionally, fault-tolerant control is implemented to maintain flight stability and prevent payload loss. Identification and removal of the damaged quadcopter from the formation preceded the execution of fault-tolerant control procedures. To simplify the research, the damaged quadcopter was predetermined.

This paper investigates fault-tolerant controls designed for multi-quadcopters that carry payloads while maneuvering. a scenario was created where several quadcopters carried a payload in a dynamic 3D environment.

The main contribution of this paper is to provide a fault-tolerant control system for multi quadcopters with suspended payloads that move in wind disturbances. The rest of this paper is organized as follows. section II describes methods, including quadcopter model, multi quadcopter with suspended payload formation control, fault-tolerant control, faulty scenario, and recovery scenario. Section III explains simulation results, and Section IV concludes this paper.

II. MATERIAL AND METHOD

A. Dynamic of Quadcopter

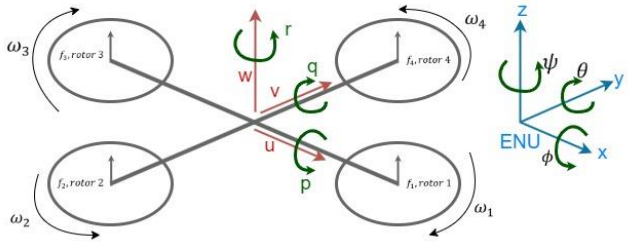

Fig. 1. Body frame and inertial frame of a quadcopter

This section explains the dynamics of the quadcopter as explained in the paper [15]. The structure of a quadcopter is explained in Figure 1 above, which corresponds to the angular velocity, torque, and force covering all four rotors. Linear position of the quadcopter is defined by inertial frame x, y, z axis by ξ. The angular angle is defined in an inertial frame with three Euler angles η. Pitch ϕ, roll θ, and yaw ψ determine rotation in x -axis, y -axis, z -axis respectively.

$$\xi = [x\ y\ z]^T; \eta = [\phi\ \theta\ \psi]^T; q = [\xi\ \ \eta]^T \quad (1)$$

Based on paper [16] dynamics of system written as:

 How to cite: Farras, A.A., Santoso, A., Nugraha, Y.E. (2024). Fault-Tolerant Control for Multi-Quadcopter with Suspended Payload under Wind Disturbance. *JAREE (Journal on Advanced Research in Electrical Engineering), 8(2).*

$$\ddot{x} = -\frac{T}{m_Q}(\cos(\phi)\sin(\theta)\cos(\psi) + \sin(\phi)\sin(\psi)) \quad (2)$$

$$\ddot{y} = \frac{T}{m_Q}(\cos(\phi)\sin(\theta)\sin(\psi) - \sin(\phi)\cos(\psi)) \quad (3)$$

$$\ddot{z} = \frac{T}{m_Q}\cos(\phi)\cos(\theta) - g \quad (4)$$

$$\ddot{\phi} = \dot{p} = \frac{(I_{yy} - I_{zz})qr}{I_{xx}} - \frac{I_r q}{I_{xx}}\omega_\Gamma + \frac{\tau_\phi}{I_{xx}} \quad (5)$$

$$\ddot{\theta} = \dot{q} = \frac{(I_{zz} - I_{xx})pr}{I_{yy}} + \frac{I_r p}{I_{yy}}\omega_\Gamma + \frac{\tau_\theta}{I_{yy}} \quad (6)$$

$$\ddot{\psi} = \dot{z} = \frac{(I_{xx} - I_{yy})pq}{I_{zz}} + \frac{\tau_\psi}{I_z} \quad (7)$$

From equations (2), (3), (4), and ξ can be rewritten into a new equation

$$\begin{bmatrix}\dot{u}\\ \dot{v}\\ \dot{w}\end{bmatrix} = \frac{T}{m_Q}R + g\begin{bmatrix}0\\0\\-1\end{bmatrix} \quad (8)$$

$$R = \begin{bmatrix}C_\psi S_\theta C_\phi + S_\psi S_\phi\\ S_\psi S_\theta C_\phi - C_\psi S_\phi\\ C_\theta C_\phi\end{bmatrix} \quad (9)$$

This quadcopter model incorporates thrust (T), rotation matrix (R), gravity acceleration (g), and quadcopter mass (m) for increased realism. Aerodynamic effects, including air drag (D) and wind force (F_w), are added to enhance the model's accuracy.

B. Air Drag and Wind Disturbance

For a more realistic response, the quadcopter experiences resistance forces and wind disturbances. Since wind disturbances and air drag directly affect all quadcopters, the model assumes these disturbances have the same value on each quadcopter.

The formula for the force produced by wind resistance is

$$f_D = \begin{bmatrix}D_x & 0 & 0\\ 0 & D_y & 0\\ 0 & 0 & D_z\end{bmatrix}\begin{bmatrix}\dot{x}\\ \dot{y}\\ \dot{z}\end{bmatrix} \quad (10)$$

where f_D is the force produced by drag, and D_x, D_y, D_z is the air drag coefficient. In addition to wind resistance, the previously described wind disturbance equation from reference [17] is incorporated, simulating a horizontal wind force acting on the quadcopter. Based on this paper, the expression of wind force is

$$f = \frac{1}{2}C\rho_{air}S\sin\theta\, v^2 \quad (11)$$

Where C is the air viscosity coefficient, ρ_{air} represents the air density, S is the surface area of the drone, and θ is the angle of the drone with the horizontal plane, v_{air} is the wind speed. According to Newton's laws, the equation reads as follows:

$$F\cos\theta = G \quad (12)$$

$$F\sin\theta - f = ma \quad (13)$$

Where m is the mass of the quadcopter and a is the acceleration created by the force combined with the drone. This model assumes a horizontal wind field, neglecting vertical wind components acting on the quadcopter formation so that with the (previous) equation then

$$\begin{bmatrix}\ddot{x}\\ \ddot{y}\\ \ddot{z}\end{bmatrix} = \begin{bmatrix}\dot{u}\\ \dot{v}\\ \dot{w}\end{bmatrix} = \frac{T}{m_Q}[R] + g\begin{bmatrix}0\\0\\-1\end{bmatrix} - \frac{1}{m_Q}F_D - \frac{1}{m_Q}F_w \quad (14)$$

Where

$$F_W = \begin{bmatrix}\frac{1}{2}C\rho_{air}S\sin\theta v^2\\ \frac{1}{2}C\rho_{air}S\sin\phi v^2\\ 0\end{bmatrix} \quad (15)$$

$$F_D = D_{air}\begin{bmatrix}u\\ v\\ w\end{bmatrix} \quad (16)$$

C. Suspended Payload System Model

In this paper there are several assumptions in lifting the load, namely: 1. The rope is attached to the midpoint of the quadcopter; 2. The charge is considered as a point mass and there are no external forces such as wind that influence it; 3) The rope is assumed to always have positive tension and without wind interference.

Quadcopters are assumed to be the same as each other and have the same payload capacity and they work together in transporting the payload to the desired place. Because each quadcopter is expected to be loaded with the same angle α, the tension of each cable is also the same. The angle α is half of the cone angle on each quadcopter. Due to the exclusion of non-standard payload configurations in this study, the payload position within the x and y planes is assumed to be the center point of the quadcopter formation. This central point will serve as the controlled position.

When the payload is suspended from the quadcopter, the position of the quadcopter that is affected by the swing of the payload can be determined as explained in the paper [18]:

$$[\ddot{\xi}] = \frac{TR}{m_Q + m_L} - \begin{bmatrix}0\\0\\g\end{bmatrix} - \frac{1}{m_Q}F_D - \frac{1}{m_Q}F_w - \frac{m_L\ddot{\rho}}{m_Q + m_L} \quad (17)$$

$\ddot{\rho}$ is the acceleration of the load with respect to the quadrotor in the inertial frame. The system dynamics for N quadcopters can be described by the following equation:

$$m_{Qi}\ddot{\xi}_{Qi} = T_i R_i - m_{Qi}\begin{bmatrix}0\\0\\g\end{bmatrix} - F_D - F_w - \frac{m_L\left(\ddot{r}_{Qi} + \ddot{\rho}_i + \begin{bmatrix}0\\0\\g\end{bmatrix}\right)}{N\cos\alpha} \quad (18)$$

where α is half of the angle formed by the quadcopter formation cone and its payload. The equation above can be transformed into the following form:

$$\ddot{\xi}_{Qi} = T_i R_i \left(\frac{N cos\alpha}{m_L + N m_{Qi} cos\alpha} \right) - \begin{bmatrix} 0 \\ 0 \\ g \end{bmatrix} - \frac{m_L \ddot{\rho}_i}{(m_L + N m_{Qi} \cos\alpha)} - \frac{1}{m_Q} F_D - \frac{1}{m_Q} [F_W] \quad (19)$$

The equation above that $\ddot{\rho}$ for each quadcopter has a different value depending on the swing produced by the disturbance. However, in this study, because it does not take into account the specific location of the payload, and the disturbances given by the quadcopter to the payload, such as changes in acceleration which affect the inertia of the payload, $\ddot{\rho}$ is assumed to always be zero while the system is running. This means that the position of the load is always just below the midpoint of the quadcopter formation.

D. Fault-Tolerant Control

Several factors require consideration when determining the formation of multiple quadcopters carrying dependent loads. These factors include the α angle and safety radius of each quadcopter. This α angle affects the thrust required by each quadcopter. The smaller the α angle, the smaller the thrust required, while the larger it is, the greater the thrust required. Several papers such as [19] use a small α angle which results in the load it carries swinging on the other hand, the paper [15] appears to use too large an α angle which is almost impossible to apply. The image below shows a comparison graph between the α angle and the force required by one of three and four quadcopters to lift a 1kg load using a rope based on Lami's theorem.

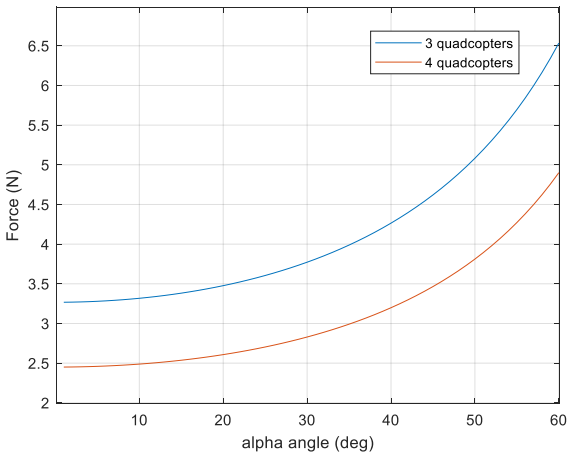

Fig. 2. Comparison between α angle and force needed to lift the payload

It can be seen that the increase in the two graphs in the figure increases exponentially. The graph above allows us to identify the maximum alpha angle achievable based on the quadcopter's lift generation capability. Consequently, this paper restricts the utilized α angle to less than 30 degrees, with the rope length adapting to maintain the quadcopter's safety radius.

Conversely, a lower alpha angle increases the likelihood of payload oscillation and necessitates closer proximity between the quadcopters, raising the risk of collisions. To mitigate this risk, a minimum safety radius is established to prevent quadcopters from entering each other's designated space. This radius is directly proportional to the quadcopter's stability; less stable quadcopters require a larger safety zone, while highly stable ones can operate with a smaller radius. Unfortunately, there's no universal formula for determining the optimal safety radius. Therefore, this paper adopts the diagonal length of the quadcopter as a conservative estimate.

Quadcopter malfunctions during operation are uncommon. However, a single damaged quadcopter can jeopardize the entire multi-quadcopter system and its payload. Therefore, enhancing multi-quadcopter formation control requires additional strategies. Determining a safe operating distance, and the safety radius is crucial before implementing fault-tolerant control systems. This radius ensures quadcopters maintain separation and prevents collisions within the formation. In this paper, there are 4 quadcopters for lifting loads. Therefore, 9 square boxes are formed where the first quadcopter is in the first box, the second quadcopter is in the third box, the third quadcopter is in the ninth box, the fourth quadcopter is in the seventh box, and finally the payload position is in the middle box, namely the fifth box. Meanwhile, the rest, namely boxes 2, 4, 6, and 8, are safety areas for quadcopters (safety regions) to prevent quadcopters from colliding with each other. Each box is set to have a side length equal to the diagonal length of the quadcopter (propeller included).

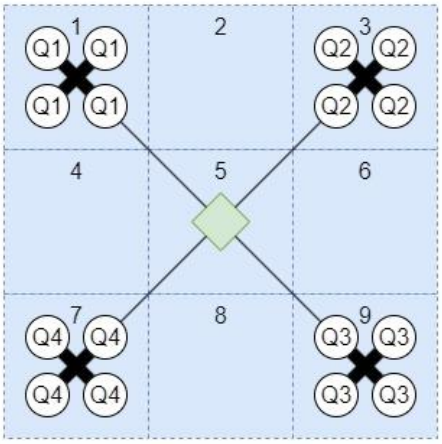

Fig. 3. Multi-quadcopter formation with suspended payload

This study examines a scenario where one of the four quadcopters carrying the payload sustains damage during flight. The analysis assumes the damaged quadcopter exerts no forces or interference on the remaining formation, simplifying the investigation. When damage occurs, the damaged quadcopter will release itself from the formation by automatically cutting the rope. Then all quadcopters will receive a signal to enter repair mode and finally perform a new formation according to the number of remaining quadcopters.

The control scheme is designed as illustrated in the following image.

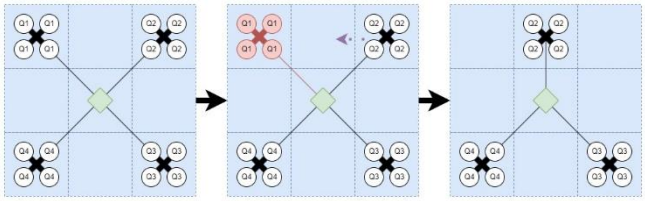

Fig. 4. Fault-tolerant control simulation

Stage 1: Malfunction detected. The N-th quadcopter that is damaged will release itself from the quadcopter formation by breaking the rope and descending from the height while remaining towards the set point.

Stage 2: Recovery mode. Select quadcopter n+1 for n=1,2,3 or Quadcopter 1 for n=4 to move 1 square closer to the position of the damaged quadcopter. On the other hand, a damaged quadcopter will be directed to the nearest goal or start position.

Stage 3: Reformation mode. All remaining Quadcopters will form an equilateral triangle formation to achieve perfect balance.

E. Quadcopter Control

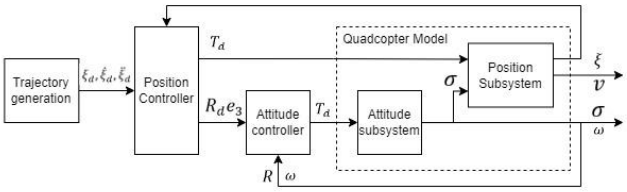

Fig. 5. Quadcopter control architecture

For quadcopter position control without a payload, a PD controller is employed due to its inherent simplicity and ease of implementation. The general form of PD control is

$$e(t) = x_d(t) - x(t)$$
$$u(t) = K_P e(t) + K_D \frac{de(t)}{dt} \quad (20)$$

where $e(t)$ is the difference between the desired position and the current position, while $u(t)$ is the signal control, K_P,and K_D are parameters for PD control.

$$T = \left(g + K_{z,P}(z_d - z) + K_{z,D}(\dot{z}_d - \dot{z})\right)\frac{m_Q}{C\phi C\theta}$$
$$\tau_\phi = \left(K_{\phi,P}(\phi_d - \phi) + K_{\phi,D}(\dot{\phi}_d - \dot{\phi})\right)I_{xx}$$
$$\tau_\theta = \left(K_{\theta,p}(\theta_d - \theta) + K_{\theta,D}(\dot{\theta}_d - \dot{\theta})\right)I_{yy} \quad (21)$$
$$\tau_\psi = \left(K_{\psi,p}(\psi_d - \psi) + K_{\psi,D}(\dot{\psi}_d - \dot{\psi})\right)I_{zz}$$

Let's assume there are 4 quadcopters used with one load hanging by a rope to the center of mass of each quadcopter. The parameters of the system are as in the table below:

TABLE I. PARAMETER OF MULTI QUADCOPTER SUSPENDED PAYLOAD SIMULATION

Parameter	Definition	Value
m_Q	UAV mass (kg)	1.2
m_L	Load mass (kg)	1
g	Gravity $\left(\frac{m}{s^2}\right)$	9.81
l	Diagonal wheelbase (m)	0.6
I_{xx}	Inertia moment of the x-axis $(kg\ m^2)$	0.03
I_{yy}	Inertia moment of the y-axis $(kg\ m^2)$	0.03
I_{zz}	Inertia moment of the z-axis $(kg\ m^2)$	0.04
A_x	Drag force coefficient of the x-axis $\left(\frac{kg}{s}\right)$	0.25
A_y	Drag force coefficient of the y-axis $\left(\frac{kg}{s}\right)$	0.25
A_z	Drag force coefficient of the z-axis $\left(\frac{kg}{s}\right)$	0.25
m_{Lmax}	Maximum load capacity (kg)	0.3
a	α angle $(deg°)$	30
L_{QL}	Cable length (m)	2
$L_{diagonal}$	Diagonal size of quadcopter (m)	0.4
Kp	Proportional gain	0.5
Kd	Derivative gain	1
C	Air viscosity coefficient	0.3
ρ_{air}	Air density $(kg/m\text{^}3)$	1.225
S	Quadcopter surface (m^2)	0.02
t_s	Time sampling (s)	0.01

The system's initial conditions are defined as a hovering state, visualized in the following image:

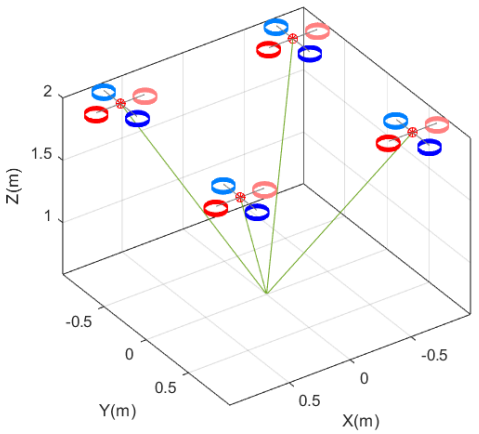

Fig. 6. Initial condition for multi-quadcopter suspended payload

Where the position of each quadcopter and payload is as follows:

$$UAV1 = [-0.7071 \quad 0.7071 \quad 2]^T$$
$$UAV2 = [-0.7071 \quad -0.7071 \quad 2]^T \quad (22)$$
$$UAV3 = [0.7071 \quad -0.7071 \quad 2]^T$$

$$UAV4 = [0.7071 \quad 0.7071 \quad 2]^T$$
$$LOAD = [0 \quad 0 \quad 0]^T$$

The n-quadcopter formation's midpoint must traverse three designated setpoints, namely

$$\begin{aligned} setpoint\ 1 &= [0 \quad 0 \quad 2\ ]^T \\ setpoint\ 2 &= [5 \quad 5 \quad 2\ ]^T \\ setpoint\ 3 &= [5 \quad 0 \quad 2\ ]^T \end{aligned} \tag{23}$$

Because each quadcopter has a position and distance that must be maintained, the setpoint for each quadcopter is obtained from the setpoint value plus offset. Where the offset is obtained by finding the distance from the center of the formation to the n-quadcopter by looking at the angle α and the length of the rope using simple trigonometry.

III. Result and Discussion

A. *Scenario 1: no fault and no wind disturbances*

Setpoints 1, 2, and 3 define the trajectory for the n-quadcopter formation's midpoint. The simulation commences with each quadcopter hovering at its respective initial position.

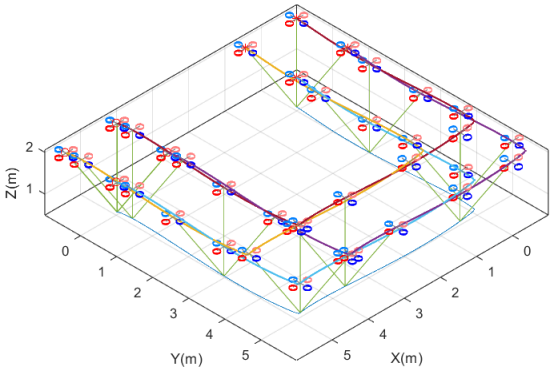

(a)

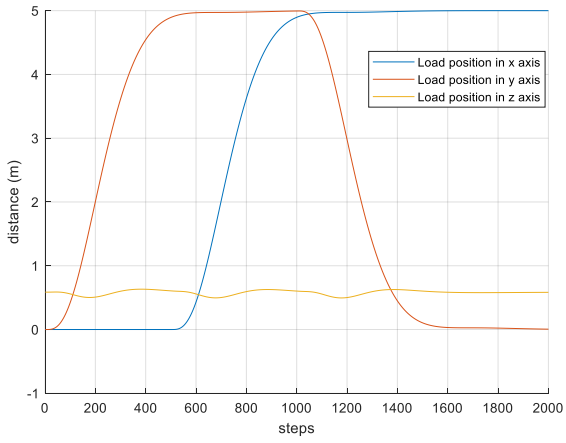

(b)

Fig. 7. Simulation multi-quadcopter with suspended payload. (a) Multi quadcopter carrying load from setpoint to another setpoint. (b) Load position in inertial frame

As shown in Fig. 7, it can be seen that the quadcopter reaches each set point within 5.2 seconds. And it can be seen that the load on the z-axis is moving up and down, this is caused by the rotational movement of the quadcopter and a slight overshoot caused by the quadcopter.

B. *Scenario 2: fault at quadcopter 1 and no wind disturbance*

This section simulates a fault scenario where Quadcopter 1 experiences a thrust reduction to 50% at the 10th second.

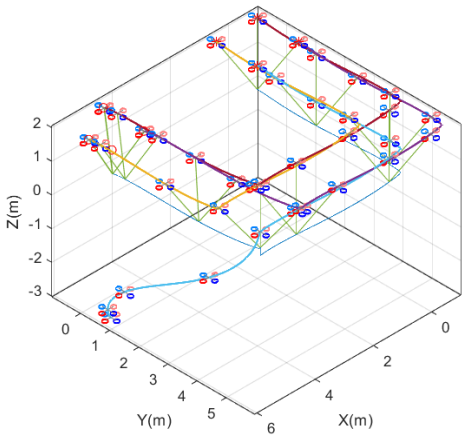

(a)

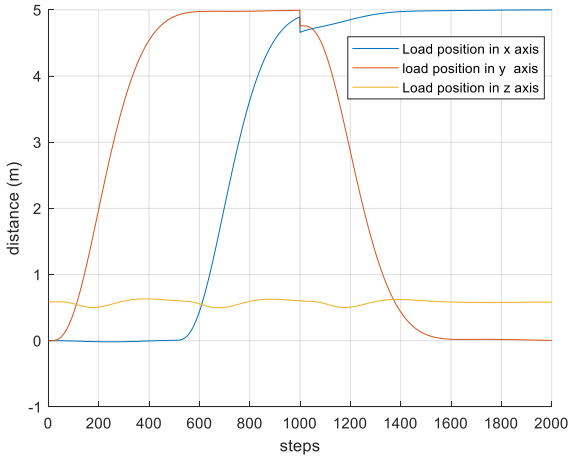

(b)

Fig. 8. Simulation of the formation control, assuming quadcopter 1 fails at the 10th second. (a) quadcopter 1 fails and the rest formation reconfigures toward a new formation. (b) Load position in an inertial frame.

When quadcopter 1 was damaged, the entire quadcopter formation system experienced a decrease in height of 6.3 cm. The position of the load is changed naturally to balance itself. And the time it takes the quadcopter to reconfigure is 3.96 seconds. Quadcopter 1 which was damaged went down to setpoint 3 because setpoint 3 was the closest distance of 5m compared to setpoint 1 which had a distance of $5\sqrt{2}m$ to quadcopter 1.

During the recovery period, it was seen that no quadcopter made a significant change in position drastically which could result information instability.

C. Scenario 3: no fault with wind distrubances

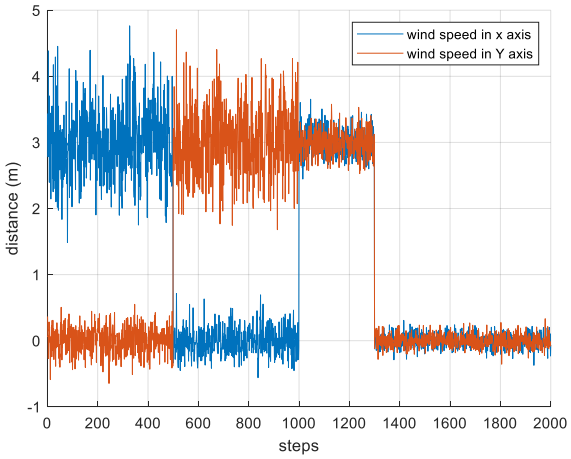

Fig. 9. Wind speed as disturbances

The simulation incorporates wind disturbances in three phases. Initially, the wind blows along the axis with a speed of and a deviation of 0.5. After an unspecified duration, the wind direction abruptly shifts to the axis for 5 seconds. Finally, for the last 3 seconds, wind blows from both the axes simultaneously, with a speed of 3 m/s and a deviation of 0.2. This three-phase wind disturbance tests the quadcopter formation's ability to maintain stability and control under varying wind conditions.

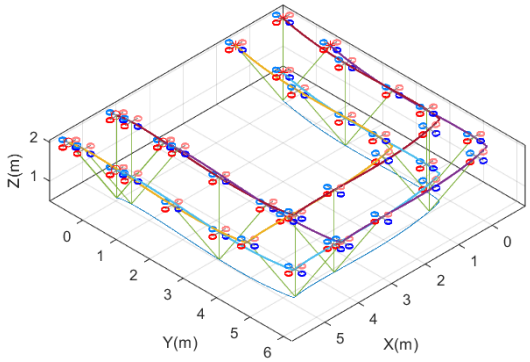

(a)

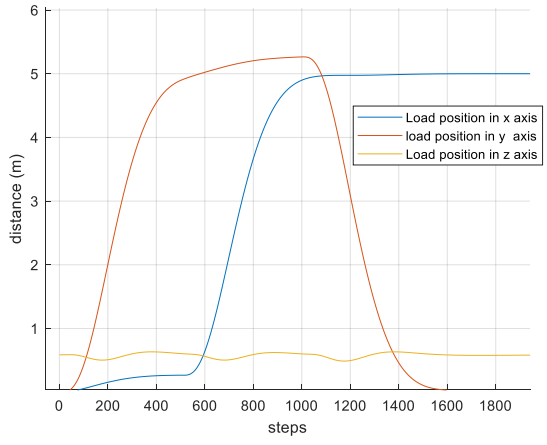

(b)

Fig. 10. (a) simulation multi-quadcopter with suspended payload under wind disturbance. (b) load position under wind disturbance.

When the quadcopter is hit by wind disturbance, the quadcopter shifts from its trajectory as far as 26cm from the direction of the wind axis.

D. Scenario 4: fault at quadcopter 1 with wind disturbance

For consistency, this scenario replicates the wind disturbances employed in scenario 3.

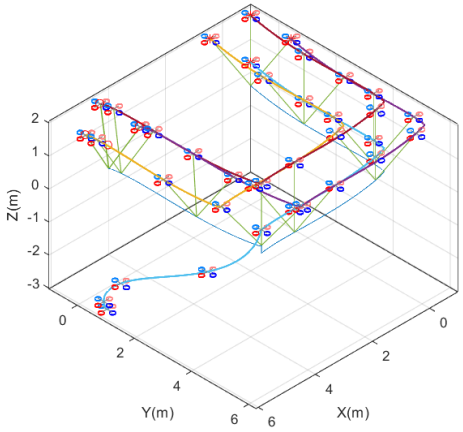

(a)

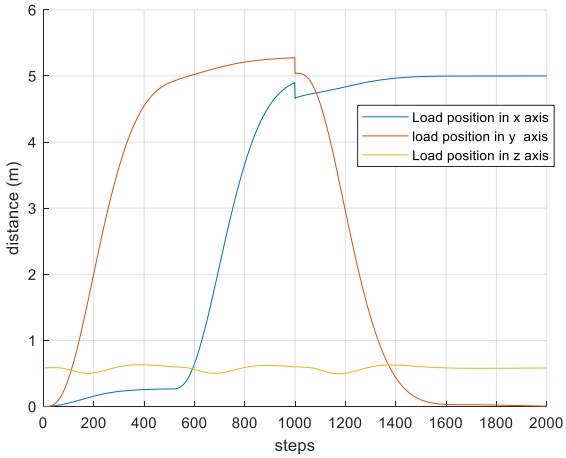

(b)

Fig. 11. (a) simulation multi-quadcopter with suspended payload under wind disturbances and faulty at quadcopter 1. (b) load position under wind disturbances and faulty at quadcopter 1.

The scenario is the same as the previous scenario 3 but there is an additional decrease in altitude caused by damage to quadcopter 1 at 10th second. Wind disturbances affect the formation position of the quadcopter with suspended payload as far as 6.3 cm. And the time it takes the quadcopter to reconfigure is 3.96 seconds.

IV. Conclusion

This paper proposes fault-tolerant control for multiple quadcopter formation systems carrying payloads. The simulation results show that when damage occurs to quadcopter 1, the position of the quadcopter does not change significantly so there is no collision between the quadcopters. Apart from that, the time required to carry out the recovery process is 3.96s. in addition, when one of the quadcopters broke away from the formation, the payload

only dropped 6.3cm. And when the quadcopter was hit by a gust of wind, the quadcopter formation only deviated by 26cm.

To achieve robust payload delivery with quadcopters, further research is crucial. We need to investigate control strategies for formations that can adapt to a variable number of drones (beyond the current limit of 4). The future research may account for other unexpected changes in quadcopter behavior (non-deterministic movement), handles situations where failures occur at unknown times, and enables dynamic formation changes beyond pre-defined patterns. By addressing these challenges, we can create a more adaptable and resilient multi-quadcopter system.

REFERENCES

[1] Chen, W. C., Lin, C. L., Chen, Y. Y., & Cheng, H. H. (2023). Quadcopter Drone for Vision-Based Autonomous Target Following. *Aerospace*, *10*(1), 82.

[2] Wu, S., Li, R., Shi, Y., & Liu, Q. (2021). Vision-based target detection and tracking system for a quadcopter. *IEEE Access*, *9*, 62043-62054.

[3] Vong, C. H., Ryan, K., & Chung, H. (2021). Trajectory tracking control of quadcopters under tunnel effects. *Mechatronics*, *78*, 102628.

[4] Habibbayli, T. H. (2022). Formation of the quadcopter flight path under overland monitoring using neuro-fuzzy modeling methods. *Mathematical machines and systems*, *3*, 97-107.

[5] Sato, R., Tanaka, K., Ishida, H., Koguchi, S., Pauline Ramos Ramirez, J., Matsukura, H., & Ishida, H. (2020). Detection of gas drifting near the ground by drone hovering over: Using airflow generated by two connected quadcopters. *Sensors*, *20*(5), 1397.

[6] Dutta, A., Chanda, A., Das, K., Das, S. C., Dwibedi, A., Bose, A., & Das, S. (2020). Self-balancing multipurpose quadcopter for surveillance system. *Int. J. Res. Appl. Sci. Eng. Technol*, *8*, 381-384.

[7] Alsoliman, A., Rigoni, G., Callegaro, D., Levorato, M., Pinotti, C. M., & Conti, M. (2023). Intrusion detection framework for invasive fpv drones using video streaming characteristics. *ACM Transactions on Cyber-Physical Systems*, *7*(2), 1-29.

[8] Siddiqui, W. A., Srivastava, M. C., Krishnan, S., & Verma, V. (2024). Design and Fabrication of FPV Racing Drone. *Journal of Mechanical and Construction Engineering (JMCE)*, *4*(1), 1-8.

[9] Hanover, D., Loquercio, A., Bauersfeld, L., Romero, A., Penicka, R., Song, Y., ... & Scaramuzza, D. (2024). Autonomous drone racing: A survey. *IEEE Transactions on Robotics*.

[10] Li, B., Li, S., Wang, C., Fan, R., Shao, J., & Xie, G. (2021, October). Distributed Circle Formation Control for Quadrotors Based on Multi-agent Deep Reinforcement Learning. In *2021 China Automation Congress (CAC)* (pp. 4750-4755). IEEE.

[11] Nurjanah, S., Agustinah, T., & Fuad, M. (2022). Cooperative position-based formation-pursuit of moving targets by multi-uavs with collision avoidance. *JAREE (Journal on Advanced Research in Electrical Engineering)*, *6*(2).

[12] Liu, H., Wang, Y., Lewis, F. L., & Valavanis, K. P. (2020). Robust formation tracking control for multiple quadrotors subject to switching topologies. *IEEE Transactions on Control of Network Systems*, *7*(3), 1319-1329.

[13] Chen, G., Peng, P., Zhang, P., & Dong, W. (2023). Risk-aware trajectory sampling for quadrotor obstacle avoidance in dynamic environments. *IEEE Transactions on Industrial Electronics*.

[14] Çorbacı, F. K., & Doğan, Y. E. (2023). An Approach to Preliminary Design of a Quadrotor Cargo UAV. *International Journal of Aviation Science and Technology*, *4*(02), 63-74.

[15] Saiella, L., Cristofaro, A., Ferro, M., & Vendittelli, M. (2021, June). Fault-tolerant formation control of a team of quadrotors with a suspended payload. In *2021 International Conference on Unmanned Aircraft Systems (ICUAS)* (pp. 1-9). IEEE.

[16] Rinaldi, M., Primatesta, S., & Guglieri, G. (2023). A comparative study for control of quadrotor UAVs. *Applied Sciences*, *13*(6), 3464.

[17] Allison, S., Bai, H., & Jayaraman, B. (2020). Wind estimation using quadcopter motion: A machine learning approach. *Aerospace Science and Technology*, *98*, 105699.

[18] Dhiman, K. K., Kothari, M., & Abhishek, A. (2020). Autonomous load control and transportation using multiple quadrotors. *Journal of Aerospace Information Systems*, *17*(8), 417-435.

[19] Klausen, K., Meissen, C., Fossen, T. I., Arcak, M., & Johansen, T. A. (2018). Cooperative control for multirotors transporting an unknown suspended load under environmental disturbances. *IEEE Transactions on Control Systems Technology*, *28*(2), 653-660.